Green Chemistry

Accepted Manuscript

www.rsc.org/greenchem

Journal Name

ARTICLE

Synthesis of 1,6-hexanediol from HMF over double-layered catalysts of Pd/SiO_2+$Ir-ReO_x/SiO_2$ in a fixed-bed reactor

Received 00th January 20xx,
Accepted 00th January 20xx

DOI: 10.1039/x0xx00000x

www.rsc.org/

Bin Xiao,[†] Mingyuan Zheng,[†]* Xinsheng Li,[†,‡] Jifeng Pang,[†] Ruiyan Sun,[†,‡] Hua Wang,[†] Xiaoli Pang,[†] Aiqin Wang,[†] Xiaodong Wang,[†] Tao Zhang[†]*

1,6-Hexanediol (1,6-HDO) was effectively prepared from 5-hydroxymethylfurfural (HMF) over double-layered catalysts of Pd/SiO_2+$Ir-ReO_x/SiO_2$ in a fixed-bed reactor. Under optimal reaction conditions (373 K, 7.0 MPa H_2, in solvent mixtures o 40% water and 60% tetrahydrofuran (THF)), 57.8% yield of 1,6-HDO was obtained. The double-layered catalysts loaded i double-layered beds showed much superior performance compared to that of a single catalyst of $Pd-Ir-ReO_x/SiO_2$, even same amount of active components were used in the catalysts. The reaction solvent significantly affected product distributions, giving a volcano-shape plot of 1,6-HDO yield as a function of the ratio of water to THF. Brønsted acidic sites were generated on the catalyst in the presence of water which played determining roles in 1,6-HDO formation. A high pressure of H_2 contributed to 1,6-HDO formation by depressing the over-hydrogenolysis of reaction intermediates and products to form hexane and hexanol. The reaction route was proposed for HMF conversion to 1,6-HDO on the basis of conditional experiments.

1. Introduction

Stimulated by ever-increasing concerns on fossil resources decline and challenges in sustainable development of economy, synthesis of high value and bulk materials from renewable feedstock has attracted great interests in the past decade.[1, 2] 1,6-Hexanediol (1,6-HDO) is a high-value and important diol with the dual hydroxyls at the molecule terminals. This structure makes it an ideal monomer for synthesis of polymers such as polyester,[3] polyurethane,[4] adhesives[5] and unsaturated polyesters.[6] Compared with widely-used polymer such as polyethylene terephthalate (PET) which is made from ethylene glycol,[7-9] polyesters made from 1,6-HDO possess superior properties in flexibility, caustic resistance and hydrolytic stability thanks to the longer carbon chain of 1,6-HDO.[10] Currently, 1,6-HDO is a petrochemical product obtained through multiple reactions including cyclohexane oxidation, esterification and hydrogenation.[10]

Catalytic conversion of biomass produces a variety of important platform chemicals, some of which are suitable to be used as precursors for synthesis of renewable monomers.[11-13] 5-Hydroymethyfurfural (HMF) is a typical versatile platform chemical that can be obtained from sugars, cellulose or lignocellulosic biomass by chemical transformations.[14-18] Besides being used for synthesis of fuels,[19, 20] it is also an important intermediate for production of polymer monomers, such as 2,5-furandicarboxylic acid,[21-23] *para*-xylene,[24, 25] and 1,6-HDO.[26-30] Buntara et al. employed 2,5-bis(hydroxymethyl)-tetrahydrofuran (DHMTHF), a product of selective hydrogenation of HMF, as feedstock for synthesis of 1,6-HDO.[26] In the presence of mixed catalysts of Nafion SAC-13 and $Rh-ReO_x/SiO_2$, 86% yield of 1,6-HDO was obtained after 20 h reaction at 120 °C. They also investigated the conversion of 1,2,6-hexanetriol (1,2,6-HTO) to 1,6-HDO with different catalysts and proposed reaction pathways.[27] Tuteja et al. developed one-pot conversion of HMF to 1,6-HDO over a Pd/ZrP catalyst using formic acid as a hydrogen source, and got 43% yield of 1,6-HDO after 21 h reaction at 413 K.[28] 2-(Hydroxymethyl)tetrahydropyran was also used as precursor for 1,6-HDO production.[26, 29, 30] The catalysts containing hydrogenation sites and acid sites, typically consisting of ReOx and noble metal Rh or Ir, are found to be effective for the selective catalytic breakage of C-O in furan ring or to obtain terminal diols from biomass.[26, 31, 32] All of these studies are accumulating much valuable knowledge and afford guidance for the synthesis of 1,6-HDO from biomass. On the other hand, the yield of 1,6-HDO is not very high yet when using HMF as feedstock (ca. 40%) to date. The reaction efficiency of these processes is low, usually needing more than 20 h to reached 100% conversion of feedstock. In addition, the reactions were conducted in batch reactors or multiple steps, the operation of which is inefficient from the point of view of industrial applications.[33] Herein, we studied the transformation of HMF to 1,6-HDO in a fixed-bed reactor. A variety of noble metal-rhenium catalysts were screened, and the effects of reaction conditions o 1,6-HDO yield were investigated. A high yield of 1,6-HDO was effectively obtained over double-layered catalysts under optimized reaction conditions. The reaction route was proposed based on the conditional experiment results. This work may provide inspiration for developing efficient catalysts and reaction systems for 1,6-HDO synthesis from biomass.

2. Experimental

2.1 Materials

HMF (99%) was provided by Ningbo Institute of Industrial Technology. Standard samples (purity>99%), including DHMTHF, 1,6-HDO, and 1,2,6-hexanetriol (1,2,6-HTO) were purchased from J&K Scientific Ltd.. Solvent of tetrahydrofuran (THF) was purchased from Tianjin Kermel Chemical Reagent Co., Ltd. Silica (99%, Qingdao Ocean Chemical Ltd., BET surface area 509 $m^2 \cdot g^{-1}$), activated carbon (99%, Beijing Guanghua-Jingke Activated Carbon Co., Ltd., BET surface area 1203 $m^2 \cdot g^{-1}$), TiO_2 (Degussa, P25), SiO_2-Al_2O_3 (Si/Al=1:7, Sinopharm Chemical Reagent Co., Ltd), HZSM-5 (Si/Al=50, The Catalyst Plant of Nankai University) and perrhenic acid (99%, Alfa Aesar) were purchased from commercial sources and used without further purification. Al_2O_3 is home-made with a surface area of 250 $m^2 \cdot g^{-1}$.

2.2 Catalyst preparation

Pd catalysts supported on different carries, including SiO_2, Al_2O_3, active carbon (AC), TiO_2, HZSM-5, SiO_2-Al_2O_3, zirconium phosphate, were prepared by incipient wetness impregnation. Taking Pd/SiO_2 as an example, 3.0 g SiO_2 was impregnated with 5.0 mL solution containing 0.14 mmol $PdCl_2 \cdot 2H_2O$ and then dried at 393 K for 12 h. After calcination at 573 K for 3 h, 0.6 wt% Pd/SiO_2 catalyst was obtained. The zirconium phosphate support was prepared as described in the literature.[28] Differing from other Pd catalysts calcined in air, the active carbon supported Pd catalyst was calcined in nitrogen atmosphere.

M-ReO_x/SiO_2 (M= Ir, Pd, Pt, Rh, or Pd-Ir, Pd-Rh) catalysts were prepared by step-wise impregnation. The M/SiO_2 was first prepared by incipient wetness impregnation with noble metal salts solutions and dried at 393 K for 12 h. Then, it was re-impregnated with an aqueous solution of perrhenic acid. After drying at 393 K for 12 h and calcination at 573 K for 3 h, the M-ReO_x/SiO_2 was obtained. For catalysts using other supports, they were prepared by the same process except the AC supported catalyst which was calcined in N_2 atmosphere.

2.3 Catalyst characterization

X-ray photoelectron spectra (XPS) were conducted on an ESCALAB 250 X-ray photoelectron spectrometer with monochromated Al Kα anode. Before experiment, the sample was reduced at 573 K in flowing hydrogen for 2 h. All binding energies were calibrated for surface charging by referencing them to the energy of the C1s peak at 284.5eV.

The metal loadings of Ir-ReO_x/SiO_2 catalysts before and after 24 h reaction were determined by inductively coupled plasma atomic emission spectrometer (ICP-AES) on an IRIS Intrepid II XSP instrument (Thermo Electron Corporation).

The FT-IR spectra of pyridine adsorption on Ir-ReO_x/SiO_2 catalyst after water vapour treatment were collected on a Bruker Equinox 55 spectrometer equipped with a deuterated triglycine sulphate (DTGS) detector in transmittance mode. In detail, the Ir-ReO_x/SiO_2 catalyst was pressed to self-supporting wafers and reduced in a H_2 stream (40 mL/min) at 573 K for 1 h. Then, it was cooled to 373 K and evacuated, followed with introduction of water vapour (saturated at ambient temperature) for 30 min. After cooling to room temperature and thorough evacuation, pyridine was absorbed until saturation. Finally, the IR cell was evacuated at 423 K and IR spectra of the sample were recorded. For comparison, FT-IR spectra of pyridine adsorption on Ir-ReO_x/SiO_2 catalyst without water treatment were measured by a similar procedure as mentioned above, except the absence of water treatment step.

2.4 Catalytic activity measurement

The catalytic conversion of HMF was conducted in a vertical fixed-bed reactor, which was made from a stainless steel tube with inner diameter of 5 mm. For evaluation of a single catalyst, 1.0 g catalyst (60-80 mesh) was loaded at the centre of reactor, and quartz granules (60-80 mesh) were filled from both sides. For evaluation of binary catalysts in the double-layered catalyst bed, 1.0 g Pd/SiO_2 was loaded at the upper layer and 1.0 g Re-based catalyst was loaded at the down layer (the two layers were separated by a thin layer of quartz wool). Prior to reaction, the catalyst was reduced at 573 K for 2 h in flowing H_2 at a rate of 60 mL/min under 3 MPa pressure. After the temperature decreased to the reaction temperature, the H_2 pressure was modulated to the desired value with a back pressure valve, and then 1% HMF solution was fed into the reactor with an HPLC pump (Model LC-20A, SHIMADZU Company) at a LHSV of 6 h^{-1} (hourly volume of reactant solution/weight of a single catalyst) in flowing hydrogen at a rate of 60 mL/min. The product solution was collected in a 100 mL tank under the reaction pressure, and periodically released for analysis. The gas products in H_2 were analysed by an in-situ gas chromatography. Typically, the results at 2 h reaction were adopted in the present contribution.

2.5 Analysis of product

The gas and liquid products were analysed with Agilent 7890B GC equipped with a Varian CP-WAX58 (FFAP) CB capillary column and HP-Plot/Q capillary column, respectively. The concentration of HMF after reaction was measured with an Agilent HPLC which was equipped with a Biorad Aminex HPX-87H organic acid column and an ultraviolet detector (Agilent G 1314 A, operated at 284 nm). The mobile phase was aqueous solution of 140 mg/L H_2SO_4 at a flow rate of 0.5 mL/min and the temperature of column was set at 318 K.

3. Results and discussion

3.1 Single catalysts screening

ReO_x based bimetallic catalysts were reported to be active for breaking C-O bond in furan ring and hydrodeoxygenation reactions.[30, 34-38] Therefore, we first synthesized a series of Re based bimetallic or tri-metallic catalysts and tested them in the one-step conversion of HMF to 1,6-HDO.

As shown in Table 1 (Entries 1-4), different noble metal-ReO_x catalysts afforded remarkably different products distribution. It should be mentioned that the solvent THF was stable in the presence of catalysts studied herein, as evidenced by the overall yield of C4 products (1,4-butanediol, butanol, or butane) lower than 0.1% on the basis of THF. The dominant product over Pd-ReO_x/SiO_2(5-5%) was DHMTHF with a high yield of 73.0% but no 1,6-HDO was formed. This suggests that Pd catalysts have high activities toward hydrogenation of aldehyde group and carbon-carbon double bonds in furan ring to form DHMTHF.[39,40] However, the catalyst showed a low activity in opening the ring of DHMTHF and did not produce 1,6-HDO. Rh-ReO_x/SiO_2 afforded 6.1% yield of 1,6-HDO. This low value is similar to that reported in the literature, where 7% yield of 1,6-HDO was obtained when using HMF as feedstock.[26] Iridium co-loaded with ReO_x showed the best performance, over which 15.2% yield of 1,6-HDO was obtained at the expense of DHMTHF yield decreased to 10.9%. Tamura et al reported that Ir-ReOx/SiO_2 was very effective to the selective hydrogenation of C=O in HMF at room temperature but not to the total hydrogenation of HMF.[41] Apparently, the reaction pathway of HMF conversion over Ir-ReOx/SiO_2 strongly depended on the reaction temperatures.

To improve the 1,6-HDO yield over Ir-ReO_x/SiO_2 catalyst, Pd was co-loaded with Ir-ReO_x based on the consideration that Pd might promote the hydrogenation of HMF and facilitate the subsequent reactions. However, the 1,6-HDO yield over Pd-Ir-ReO_x/SiO_2(0.6-5-5) (Table 1, Entry 5) turned out to be very similar to that of Ir-ReO_x/SiO_2(5-5) (14.6% vs. 15.2%), and gave significant amount of 1,2,6-HTO (30.4% yield). Increasing Pd loading to 5% led to slight improvement of 1,6-HDO yield to 19.2%, accompanied with notable increase in the by-product of 1,5-HDO (Entry 6). These results suggest that Pd, Ir, and ReO_x could be used as effective active components for the 1,6-HDO preparation from HMF, but the product selectivity over them needs to be improved through rational design of catalysts and optimization of reaction conditions.

In addition, it was found that catalyst supports affected the product selectivity significantly. Differing from SiO_2 supported catalysts, active carbon supported Ir-ReO_x did not produce 1,6-HDO (Table 1, Entry 7) but formed 36% yield of 2-hexanol and much unknown products which were undetectable by GC or HPLC analysis. ZrP and Al_2O_3 supported catalysts did not give a high yield of 1,6-HDO either. Since the SiO_2 supported catalysts showed the best performance for HMF conversion to 1,6-HDO, they were further studied in the following sections.

3.2 Screening of catalysts in a double-layered catalyst bed

Now that using a single catalyst met great challenges in effectively coupling the multiple reactions of HMF conversion to 1,6-HDO, we further employed binary catalysts and loaded them in double layers to improve the selectivity of 1,6-HDO. The catalyst at upper layer would primarily take charge of hydrogenation of HMF, and the catalyst at the down layer fulfills the function of subsequent hydrogenolysis of furan ring to 1,6-HDO. It was reported that Pd based catalyst could transformed HMF to DHMTHF with high selectivity.[42] Therefore, the Pd catalysts supported on different carriers were first screened for obtaining a high selectivity. As shown in Figure 1, Pd/SiO_2(0.6%) catalyst showed the highest selectivity (86%) toward DHMTHF with 13% hexane formation at 373 K. Increasing palladium loading from 0.6 to 5% did not improve DHMTHF selectivity over the Pd/SiO_2. The yield of DHMTHF over Pd/Al_2O_3 was slightly lower than that on Pd/SiO_2. In contrast, over Pd/AC catalyst, besides the formation of DHMTHF and hexane, 22% yield of MHMTHF was also produced, which is the hydrodeoxygenation product of DMHTHF. Over acidic carries of SiO_2-Al_2O_3 and HZSM-5 supported Pd catalysts, the yield of DHMTHF was rather low with significant loss in carbon balance due to formation of undetectable products. The Pd/TiO_2 afforded the worst performance without any DHMTHF production. Taken all together, 0.6% Pd/SiO_2 catalyst was the best one to be used as the upper-layer catalyst in the following study.

Table 1. Product yields in HMF hydrogenolysis over different catalysts[a].

Entry	Catalysts	1,6-HDO/%	2,5-HDO/%	1,5-HDO/%	Hexane/%	1-Hexanol/%	DHMTHF/%	MHMTHF/%	1,2,6-HTO/%
1	Pd-ReO_x/SiO_2(5-5)	0	0	0	8.0	0	72.9	8.4	0
2	Pt-ReO_x/SiO_2(5-5)	2.3	0	4.6	23.9	0	32.6	9.1	0
3	Rh-ReO_x/SiO_2(5-5)	6.1	0	0	13.3	0	42.9	0	28.1
4	Ir-ReO_x/SiO_2(5-5)	15.2	0	13.7	18.2	11.7	10.9	0	12.2
5	Pd-Ir-ReO_x/SiO_2(0.6-5-5)	14.6	0	11.5	8.5	0	18.8	6.4	30.4
6	Pd-Ir-ReO_x/SiO_2 (5-5-5)	19.1	0	22.0	24.6	4.0	6.8	2.7	0
7	Ir-ReO_x/AC(5-5) *	0	0	0	14.2	36.0	0	0	0
8	Ir- ReO_x/ZrP(5-5)**	4.8	0	0	13.5	0	0	5.0	0
9	Ir- ReO_x/Al_2O_3(5-5)***	0	0	0	14.8	0	42.1	10.5	6.0

[a] Reaction condition: 373 K, 3 MPa H_2, 1.0 g catalyst loaded in the fixed-bed reactor, mixture solvents of water and THF at volume ratio of 2:3, 1 wt% HMF, LHSV=6 h^{-1}. HMF conversions were 100% in all experiments.

* Ir-ReO_x/C(5-5) gave product of 2-hexanol but not 1-hexanol; ** Ir-ReO_x/ZrP(5-5) gave large amount of unknown precipitate; *** Ir-ReO_x/Al_2O_3(5-5) gave product of dihydroxylfurfuran but not DHMTHF.

Denote: 1,6-HDO, 2,5-HDO, 1,5-HDO, DHMTHF, MHMTHF, and 1,2,6-HTO represent 1,6-hexanediol, 2,5-hexanediol, 1,5-hexanediol, 2,5-bis(hydroxymethyl)-tetrahydrofuran, 5-methyltetrahydrofurfuryl alcohol, and 1,2,6-hexanetriol, respectively.

Table 2 lists the results of HMF transformation over different double-layered catalysts in the fixed-bed reactor. Compared to the performance of single catalysts listed in Table 1, the 1,6-HDO yield was significantly improved. Over double-layered catalysts of Pd/SiO_2(0.6)+Ir-ReO_x/SiO_2(5-5), 36.1-46.0% yield of 1,6-HDO was obtained (Table 2, Entries 1,2) in contrast to 14.6% yield of 1,6-HDO (Table 1, Entry 5) over the single catalyst of Pd-Ir-ReO_x/SiO_2(0.6-5-5), even though the same loadings of active components were used in both cases. In addition, the performance of Ir-ReO_x/SiO_2(5-5) is notably superior to that of Rh-Re/SiO_2(5-5) (9.7% yield, Table 2 Entry 3), which was reported to be active for 1,6-HDO production from DHMTHF.[26] The inferior performance of Rh-Re/SiO_2 might result from no use of acidic catalyst such as Nafion SAC-13 in the present study.

The 1,6-HDO yield over Pd/SiO_2(0.6)+Ir-ReO_x/SiO_2 first increased and then levelled off at 46.0% with the ReO_x loading increasing from 0.5 to 5%, accompanied with the decrease of DHMTHF yield from 11.4 to 1.4% (Table 2, Entries 1, 4-6). This indicates that ReO_x played an important role in selectively catalyzing the ring opening of DMHTHF, which is consistent with the findings in literatures.[26, 29-32, 38] In addition, the ReO_x slightly contributed to the hexane formation as evidenced by more hexane formed with the increase of ReO_x loading.

The support of Ir-Re catalysts had remarkable effects on the product selectivity. Compared to the SiO_2 supported catalyst, Al_2O_3 and activate carbon supported Ir-Re catalysts gave much lower yields of 1,6-HDO but more DHMTHF formation. Zirconium phosphate supported palladium catalysts were recently reported to be active for the HMF transformation to 1,6-HDO.[28] However, the Ir-ReO_x/ZrP in combination with Pd/SiO_2(0.6) did not produce 1,6-HDO, and the primary products were DHMTHF at a high yield of 73.8% (Table 2, Entry 7). This suggests that the activity of Ir-ReO_x/ZrP catalyst for ring-opening of tetrahydrofuran is very low. Tuteja et al,

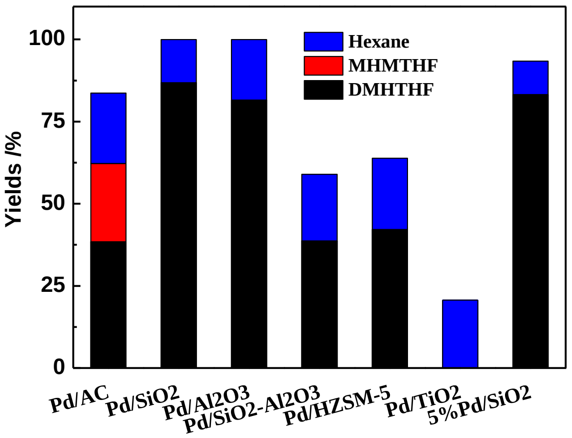

Figure 1. Results of HMF hydrogenation over Pd catalysts supported on different carries, the loadings of palladium in all catalysts were 0.6 wt% except 5% Pd/SiO_2. (HMF conversions were 100% in all experiments; Reaction conditions: 373 K, 3 MPa H_2, mixed solvents of water and THF at volume ratio of 2:3, 1 wt% HMF, LHSV=6 h^{-1}).

Table 2. Products yields in HMF hydrogenolysis over double-layered catalysts[a]

Entry	Catalysts	1,6-HDO/%	1,5-HDO/%	Hexane/%	1-Hexanol/%	DHMTHF/%	MHMTHF/%
1	Pd/SiO_2(0.6)+Ir-ReO_x/SiO_2(5-5)	46.0	18.1	10.0	24.3	1.4	0
2	Pd/SiO_2(0.6)+Ir-ReO_x/SiO_2(5-5)[b]	36.1	15.0	25.3	16.8	0	
3	Pd/SiO_2(0.6)+Rh-ReO_x/SiO_2(5-5)	9.7	9.8	20.8	0	35.6	0
4	Pd/SiO_2(0.6)+Ir-ReO_x/SiO_2(5-2.5)	46.2	19.4	12.9	17.5	4.7	0
5	Pd/SiO_2(0.6)+Ir-ReO_x/SiO_2(5-1)	39.4	11.7	4.5	8.7	7.3	0
6	Pd/SiO_2(0.6)+Ir-ReO_x/SiO_2(5-0.5)	28.7	10.3	6.3	11.3	11.4	0
7	Pd/SiO_2(0.6)+Ir-ReO_x/ZrP (5-5)	0	0	22.5	0	73.8	7.2
8	Pd/SiO_2(0.6)+Ir-ReO_x/C(5-5)	8.2	8.6	23.6	3.5	35.5	0
9	Pd/SiO_2(0.6)+Ir-ReO_x/Al_2O_3(5-5)	15.9	9.3	15.9	0	30.0	0

[a] Reaction condition: 373 K, 5 MPa H_2, 1.0 g Pd/SiO_2 loaded at the upper layer and 1.0 g Re-based catalyst loaded at the down layer, mixture solvents of water and THF at volume ratio of 2:3, 1 wt% HMF, LHSV=6 h^{-1} based on amount of single catalyst. HMF conversions were 100% in all experiments.

Pd/SiO_2(0.6)+Ir-ReO_x/SiO_2(5-5)[b] was evaluated under 3 MPa H_2.

1,6-HDO, 1,5-HDO, DHMTHF, and MHMTHF represent 1,6-hexanediol, 1,5-hexanediol, 2,5-bis(hydroxymethyl)-tetrahydrofuran and 5-methyltetrahydrofurfuryl alcohol, respectively.

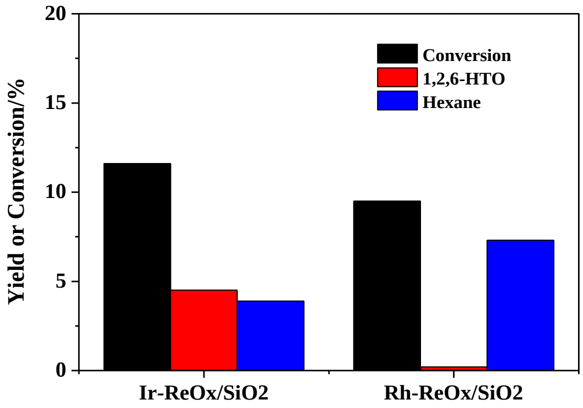

Figure 2. Results of DHMTHF hydrogenolysis over Ir-ReO$_x$/SiO$_2$(5-5) and Rh-ReO$_x$/SiO$_2$(5-5) catalysts in a batch reactor, each metal loading on catalysts is 5 wt%. (Reaction conditions: 20 h, 373 K, 5 MPa H$_2$, 0.15 g catalyst, 20 mL 1% DHMTHF in mixed solvents of water and THF at volume ratio of 2:3).

proposed that over ZrP supported catalysts, HMF was transformed to 1,6-HDO through six-step reactions and an intermediate of hex-1,3,5-triene-1,6-diol.[28] This mechanism would be quite different from that over the Pd/SiO$_2$(0.6)+Ir-ReO$_x$/SiO$_2$ studied herein.

It should be noted that the catalysts loaded in the double-layered fixed-bed reactor exhibited remarkably superior performance compared to that in a batch reactor. As shown in Figure 2, when DHMTHF (the product of HMF hydrogenation over Pd/SiO$_2$) was used as feedstock in a batch rector in the presence of Ir-ReO$_x$/SiO$_2$(5-5) or Rh-ReO$_x$/SiO$_2$(5-5), the conversions of DHMTHF were less than 20%. The main product was 1,2,6-HTO and hexane without 1,6-HDO formation even after 20 h reaction. This suggests that the conversion of DHMTHF was increased by ca. 5 folds together with high selectivity to 1,6-HDO in the fixed-bed reactor as compared with that in a batch reactor.

3.3 Effect of solvent on 1,6-HDO production

The choice of the reactant solvent is an important factor that often remarkably affects the products distribution.[43-45] Two kinds of solvent, i.e., protic solvent of water and aprotic solvent of tetrahydrofuran (THF), were used at different mixture ratios for the HMF transformation. As shown in Figure 3, when pure THF was used as the reaction solvent, the dominant product was DHMTHF (76.8% yield) accompanied with 21.7% yield of hexane, but no 1,6-HDO was formed. In contrast, in pure water solution, the primary products were 1,6-HDO and hexanol (20.9% and 25.3% yields, respectively), while the yield of DHMTHF decreased nearly to zero. Tuning the ratio of THF to water led to a volcano-shape curve of 1,6-HDO yield, which gave the maximum value of 36.1% at 40% water content in the THF solution. A suitable ratio of THF to water benefited HMF conversion to 1,6-HDO. Considering pure aqueous solution would be detrimental to the stability of silica supported catalysts due to gradual collapse of the silica support under hydrothermal environment, the mixed solvent containing 40% water and 60% THF was used as a typical reaction medium in the present study.

As for the reason why the 1,6-HDO selectivity was dramatically different between using THF and water as the solvent, there still lacks very clear understanding. For the performance of upper layer catalyst of Pd/SiO$_2$ in HMF conversion in different solvents, no big difference was observed with yields of DHMTHF ranging from 89% to 100% (Figure 4). Therefore, the different selectivity of 1,6-HDO should be primarily ascribed to the effect of solvent on the catalytic conversion of DHMTHF over the down layer Ir-ReO$_x$/SiO$_2$ catalyst.

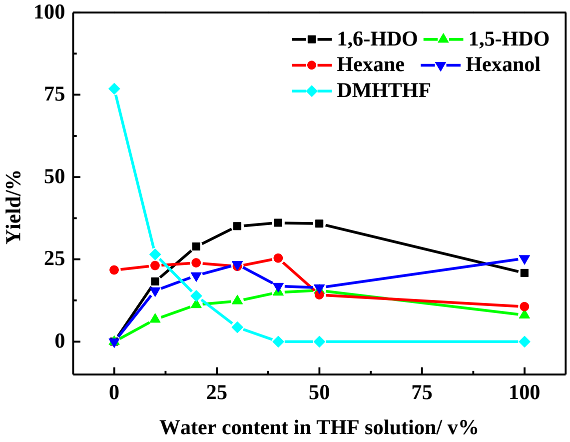

Figure 3. Effect of water content in the THF solution on the product yields over Pd/SiO$_2$(0.6%)+Ir-ReO$_x$/SiO$_2$ (5%-5%) catalysts. (HMF conversions were 100% in all experiments; Reaction condition: 373 K, 3 MPa H$_2$, 1 wt% HMF, LHSV=6 h^{-1}).

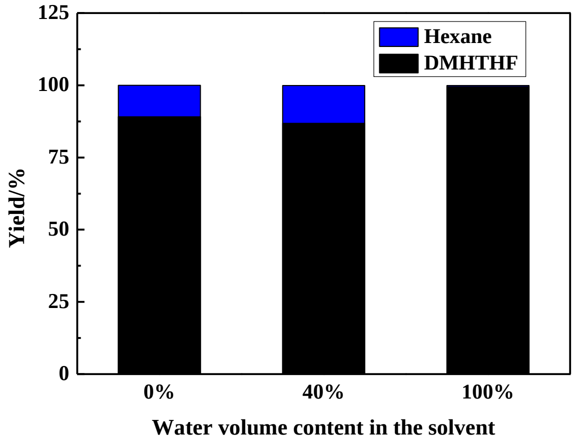

Figure 4. Effect of water content in the THF solution on HMF conversion to DHMTHF over the upper-layer catalyst of Pd/SiO_2(0.6) without Ir-ReO_x/SiO_2. (HMF conversions were 100% in all experiments; Reaction condition: 373 K, 3 MPa H_2, HMF concentration was 1 wt%, LHSV=6 h^{-1}).

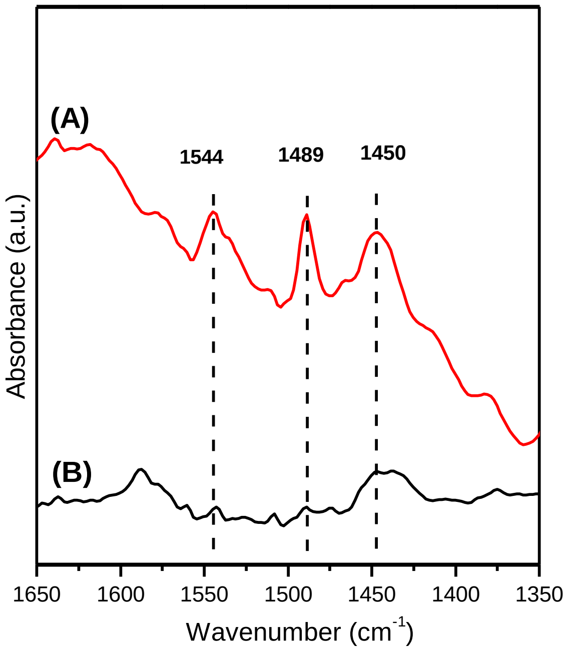

Figure 5. FT-IR spectra of pyridine adsorbed on Ir-ReO_x/SiO_2(5-5) catalyst: (A) catalyst treated with water vapour; (B) catalyst without water treatment.

The acidic property of Ir-ReO_x/SiO_2 catalyst was probed by IR spectroscopy of pyridine adsorption. As shown in Figure 5, the characteristic peaks occurred at 1450 cm^{-1} and 1544 cm^{-1} belong to Lewis and Brønsted acidic sites, respectively.[46,47] The peak at 1489 cm^{-1} is associated with both Brønsted and Lewis acids.[48] It can be noticed that Brønsted acidic sites were significantly generated on the Ir-ReO_x/SiO_2 catalyst after the pretreatment with water vapour. The XPS characterization disclosed that a remarkable portion (ca. 30%) of Re existed in oxide forms of Re^{4+} on the Ir-ReO_x/SiO_2, whic could account for the origin of acidic sites (Figure 6). The STEM and EDX images demonstrated that Ir and Re elements had very similar distribution on the silica support, suggesting that Ir and R coexisted closely (Supporting information Figure S1). Chia et al studied the selective hydrogenolysis of secondary C–O bonds for a wide range cyclic ethers and polyols over ReO_x-Rh/C catalyst.[38] They found that the catalyst realized selective hydrogenolysis of C–O bonds by acid-catalyzed ring-opening and dehydration reactions coupled with metal-catalyzed hydrogenation. The hydroxyl groups on Re atoms associated with metallic Rh are acidic.[38] Tomishige's group studied the Re-modified Ir catalyst and identified that Ir metal particles were modified with ReO_x clusters regardless the catalyst being used in water or *n*-heptane solvent or freshly reduced in dry conditions.[49-51] Also, they proposed that the protonic acid participated in the catalytic ring opening of tetrahydrofuran.[5 Taken all together, it is rational to conjecture that ReO_x species on Ir-ReO_x/SiO_2 are partially hydrolyzed in the presence of water to produce hydroxyl groups on the surface, which provide Brønsted acidic sites for the catalytic opening of furan ring of DHMTHF. In contrast, in THF, a non-protonic organic solvent, the amount of hydroxyl groups on ReO_x surface would be much less, which led to the low activity of DHMTHF conversion (lower than 25%). In addition, as reported by Nakagawa et al, alcohol reactants in alkane solvent could adsorb on Ir-ReO_x/SiO_2 catalyst more strongly than that in water.[49] Therefore, in the mixed solvents of THF and water, the abundant amount of Brønsted acidic sites and possibly suitable adsorption strength of reactants could account for the maximum yield of 1,6-HDO in HMF conversion.

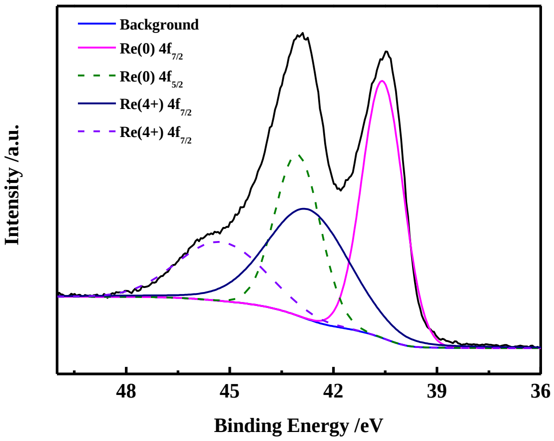

Figure 6. XPS spectra of Ir-ReO_x/SiO_2(5%-5%) catalyst.

3.4 Effect of hydrogen pressure on products distribution

As shown in Figure 7, the H_2 pressure significantly affected the product distributions. The yield of 1,6-HDO was merely 11.8% but hexane yield reached 76.3% at 0.5 MPa H_2. Increasing H_2 pressure to 7 MPa greatly improved the yield of 1,6-HDO to 57.8% while depressed hexane yield to 8.6%. The yield of hexanol first increased from zero to 24% and then decreased to 8.2% with H_2 pressure increasing. The high pressure of hydrogen seems to inhibit the further hydrogenolysis of 1,6-HDO to form hexanol and hexane.

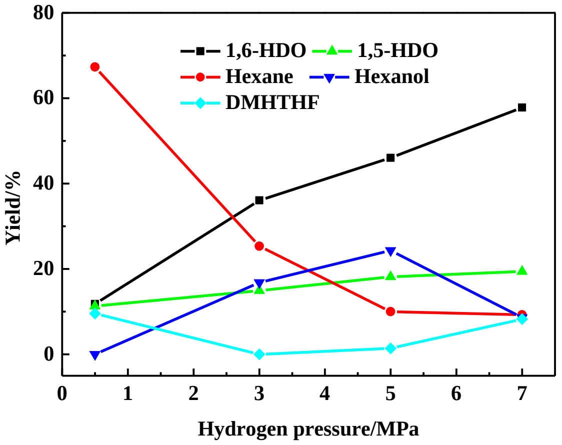

Figure 7. The products distribution under different hydrogen pressures over Pd/SiO_2(0.6%)+Ir-ReO_x/SiO_2(5%-5%) catalysts. (HMF conversions were 100% in all experiments; Reaction condition: 373 K, mixed solvents of water and THF at volume ratio of 2:3, 1 wt% HMF, LHSV=6 h^{-1}).

To identify the reasons for the promoting effect of H_2 pressure on 1,6-HDO formation, the catalytic performance of upper-layer catalyst Pd/SiO_2 was tested. As shown in Figure 8, the H_2 pressure also imposed notable promoting effects on DMHTHF formation over Pd/SiO_2. With the hydrogen pressure increasing from 0.5 to 7 MPa, DMHTHF yield was enhanced from 57 to 94% along with a remarkable decrease in hexane yield. Correlating the yield of DMHTHF in HMF conversion over the upper-layer Pd/SiO_2(0.6%) catalyst (Figure 8) and the yield of 1,6-HDO over the double-layered catalysts (Figure 7), the net selectivity of 1,6-HDO in DMHTHF conversion over the down-layer Ir-ReO_x/SiO_2 (5%-5%) catalyst was obtained (Figure 9). Evidently, H_2 pressure imposed a remarkably positive effect on the selectivity of 1,6-HDO in DMHTHF conversion. Meanwhile, hexane yield decreased with the increase of H_2 pressure over the down layer catalyst.

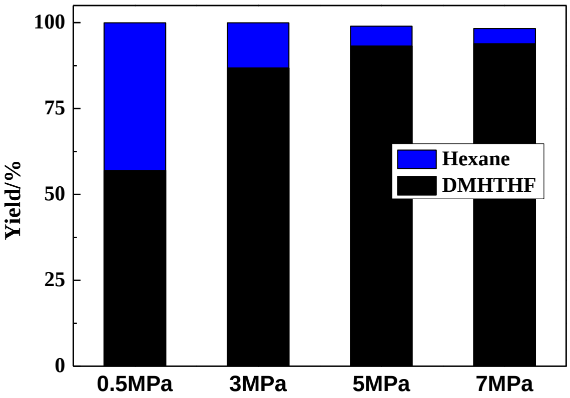

Figure 8. Effect of hydrogen pressure on the product distribution over Pd/SiO_2(0.6%) catalyst (HMF conversions were 100% in all experiments; Reaction condition: 373 K, mixed solvents of water and THF at volume ratio of 2:3, 1 wt% HMF, LHSV=6 h^{-1}).

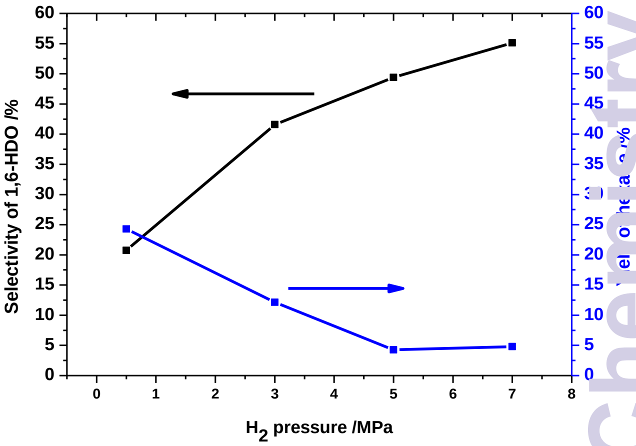

Figure 9. Net selectivity of 1,6-HDO and net yield of hexane in DMHTHF conversion over the down layer catalyst of Ir-ReO_x/SiO_2(5%-5%) under different hydrogen pressures. (The net selectivity of 1,6-HDO was obtained by dividing 1,6-HDO yields in Figure 7 by DMHTHF yields in Figure 8; The net yield of hexane was obtained by subtracting the yields in Figure 7 with the yields in Figure 8).

It was reported that competitive adsorption between hydrogen and reactant on the catalyst surface could depress the hydrogenolysis.[53] With the increase of H_2 pressure, more hydrogen would occupy the metallic active sites and eliminate the coverage of DHMTHF and 1,6-HDO on the upper-layer Pd/SiO_2 catalyst and the down-layer $Ir\text{-}ReO_x/SiO_2$ catalyst, respectively, which consequently decreased the over-hydrogenolysis of 1,6-HDO to form hexane. In addition, as mentioned in section 3.2, ReO_x sites played roles in hexane formation. Therefore, it can be conjectured that 1,6-HDO should be formed at the interfacial sites between ReO_x and hydrogenation metal sites, which is in agreement with the conclusion reported by Dumesic et al.[38] A high pressure of H_2 would contribute to the removal of 1,6-HDO from active sites and decrease the opportunity of the further hydrodeoxygenation of 1,6-HDO to hexane.

3.5 Route for the conversion of HMF to 1,6-HDO

The reaction route of HMF conversion to 1,6-HDO was probed by varying reaction temperatures and conditional experiments. As shown in Figure 10, the main product was 1,2,6-HTO at a yield of 42.4% yield at 333 K, accompanied with 27% yield of DHMTHF and 22% yield of 1,6-HDO. Increasing temperature led to continuous decreasing of 1,2,6-HTO and DHMTHF yields, while the yield of 1,6-HDO raised to the highest value of 46% at 373 K. Similarly, as space velocity of the reaction was increased two and five times, the yield of 1,6-HDO decreased but the yields of 1,2,6-HTO and DHMTHF increased remarkably (Supporting information Figure S2). These results strongly suggested that the 1,6-DHO formation underwent intermediates of DHMTHF and 1,2,6-HTO. In addition, as shown in Figure 8, over the upper layer Pd/SiO_2 catalyst HMF was converted to DHMTHF at a yield of 86%. Therefore, it can be inferred that DHMTHF was converted over the down layer $Ir\text{-}ReO_x/SiO_2$ catalyst to form 1,2,6-HTO which acted as the precursor of 1,6-HDO. The conditional experiment show that when 1,2,6-HTO was used as the reaction substrate, 54% yield of 1,6-HDO was obtained, further confirming that 1,2,6-HTO is the precursor of 1,6-HDO (Figure 11).

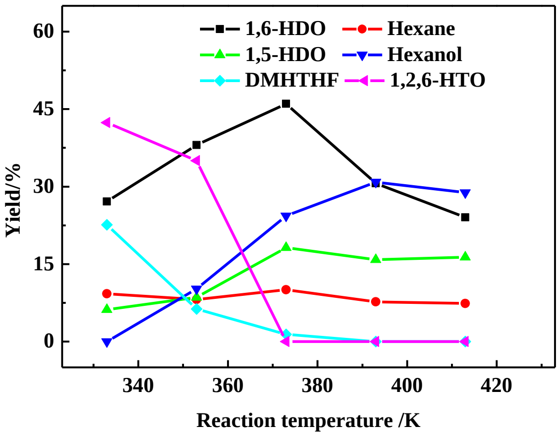

Figure 10. Effects of reaction temperature on the products distribution for HMF conversion to 1,6-HDO over $Pd/SiO_2(0.6\%)+Ir\text{-}ReO_x/SiO_2(5\%\text{-}5\%)$ catalysts. (HMF conversions were 100% in all experiments; Reaction condition: 5 MPa H_2, mixed solvents of water and THF at volume ratio of 2:3, 1 wt% HMF, LHSV=6 h^{-1}).

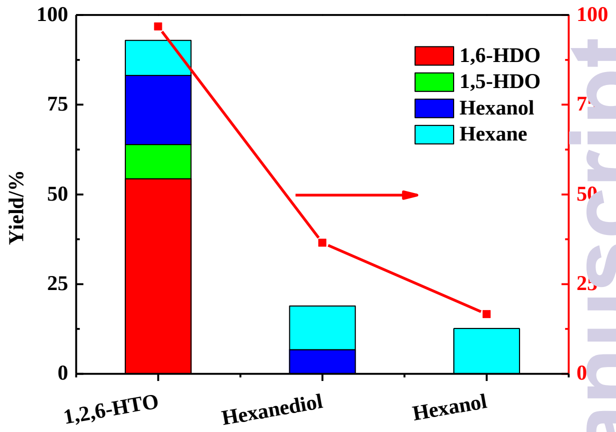

Figure 11. Results of hydorgenolysis of typical intermediates over Ir-ReO_x/SiO_2 catalyst. (Reaction condition: 373 K, 3 MPa H_2, mixed solvents of water and THF (H_2O:THF = 2:3/v:v), reactant concentrations were all 1 wt%, LHSV=6 h^{-1}).

The main byproducts in HMF conversion to 1,6-HDO were 1,5-HDO, hexanol and hexane. At 373 K, the ratio of 1,5-HDO yield to 1,6-HDO yield was 2/5 in the HMF conversion over the double-layered catalysts $Pd/SiO_2(0.6\%)+Ir\text{-}ReO_x/SiO_2(5\%\text{-}5\%)$ (Table 2, entry 1). The conditional experiment showed that 1,5-HDO can be produced in 1,2,6-HTO conversion (Figure 11), but the its yield was merely 1/6 of that of 1,6-HDO, notably lower than 2/5 in the case of HMF conversion. Therefore, besides formed from 1,2,6-HTO, nearly half amount of 1,5-HDO was formed from other precursors, possibly from 5-methyltetrahydrofurfuryl alcohol which is a hydrodeoxygenation product of DHMTHF.

As for the byproduct hexanol, on one hand it could be derived from 1,6-HDO. As shown in Figure 11, 6.7% yield of hexanol was obtained when using 1,6-HDO as the reactant. On the other hand, hexanol could also be produced from other polyols, such as 1,5-HDO, according to the fact that the yield of hexanol (16.8%) in HMF conversion is higher than that of hexanol (6.7%) obtained in 1,6-HDO conversion.

Besides, it should be noted that although 1,6-HDO could be hydrodeoxygenated to hexane and hexanol, the conversion of 1,6-HDO was much lower than the conversions of HMF and 1,2,6-HTO. This suggests that the 1,6-HDO is more stable than other reaction intermediates over the $Ir\text{-}ReO_x/SiO_2$ catalyst, which is a virtue for obtaining 1,6-HDO at a high yield in HMF conversion.

According to the above analysis, the reaction routes of HMF conversion to 1,6-HDO were proposed and shown in Scheme 1.

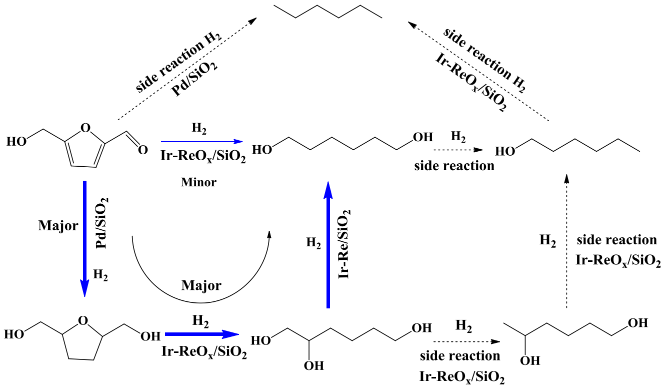

Scheme 1. Reaction routes of HMF conversion to 1,6-HDO over Pd/SiO$_2$+Ir-ReO$_x$/SiO$_2$ catalysts.

3.6 Catalyst stability

The stability of the optimized catalysts was tested and the results are shown in Figure 12. The yield of 1,6-HDO was ca. 60% at beginning and maintained at higher than 50% during 15 h reaction. After 24 h running, the 1,6-HDO yield slightly decreased to ca. 40%, accompanied with the yields of hexanol and 1,5-HDO decreasing. Conversely, the yield of 1,2,6-HTO significantly increased from zero to 42% after 24 h reaction. As discussed above, 1,2,6-HTO was the precursor of 1,6-HDO, and its conversion was closely related to the ReO$_x$ species on the catalyst. Elemental analysis showed that loadings of Ir or Pd on the Ir-ReOx/SiO$_2$ and Pd/SiO$_2$ catalysts did not changed before and after reaction. However, the ReO$_x$ loading decreased from 5% to 3% on the spent catalyst. This is consistent with a previous report that Re oxides could leach into the solution in the long time running.[38] In addition, comparing the surface areas and pore size distributions of the catalysts before and after usage, no big difference was found (ca. 400 ± 20 m^2/g, 5.6 ± 0.1 nm). It is can be concluded that the loss in 1,6-HDO was mainly caused by the leach of Re during the reaction. Therefore, for the practical application, the stability of catalyst needed to be further improved by optimizing preparation method or using more stable active components for the catalyst.

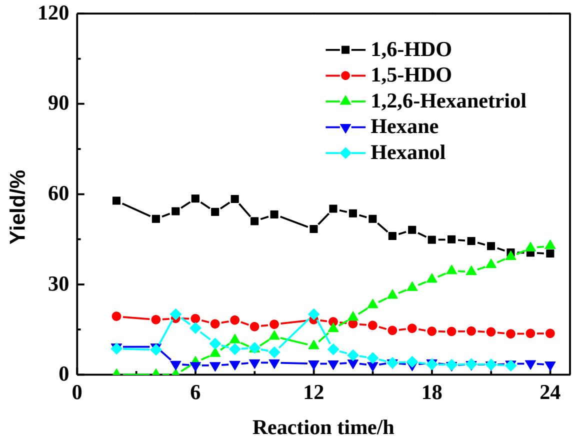

Figure 12. Results of stability evaluation of Pd/SiO$_2$(0.6%)+Ir-ReO$_x$/SiO$_2$(5%-5%) catalysts. (HMF conversion was 100%; Reaction condition: 373 K, 7 MPa H$_2$, mixed solvents of water and THF at volume ratio of 2:3, 1 wt% HMF, LHSV=6 h^{-1}).

4. Conclusions

In summary, biomass-derived HMF was effectively converted into 1,6-HDO over double-layered catalysts in a fixed-bed reactor. Under optimal reaction conditions of 373 K and 7 MPa H$_2$, 57.8% yield of 1,6-HDO was obtained over Pd/SiO$_2$+Ir-ReO$_x$/SiO$_2$. The double-layered composite catalyst showed much superior performance in improving the target product selectivity as compared with a single catalyst. The reaction solvent significantly effected 1,6-HDO formation, and mixed solvents of water and THF at volume ratio of 2:3 was the most suitable to afford an enhanced 1,6-HDO yield. A high pressure of H$_2$ contributed to the formation of 1,6-HDO by depressing the over-hydrogenolysis of reaction intermediates and products to form hexane and hexanol. According to the results of conditional experiments, the reaction route was elucidated, wherein DHMTHF and 1,2,6-HTO were the successive intermediates for the formation of 1,6-HDO. The Pd/SiO$_2$+Ir-ReO$_x$/SiO$_2$ catalysts showed reasonably good stability with 1,6-HDO yield in a range of 60% to 40% in 24 h running. The catalyst deactivation was attributed to the gradual leaching of ReO$_x$ during the reaction.

Acknowledgements

This work was supported by the National Nature Science Foundation of China (21376239, 21306191).

Notes and references

[†]Dalian Institute of Chemical Physics, Chinese Academy of Sciences, State Key Laboratory of Catalysis, Zhongshan Road 457, Dalian 116023, China.

[‡]Graduate University of Chinese Academy of Sciences, Beijing 100049, China.

*Corresponding author: Tel.: +86 411 84379738; fax: +86 411 84691570;

E-mail address: myzheng@dicp.ac.cn; taozhang@dicp.ac.cn.

1. G. W. Huber, S. Iborra and A. Corma, *Chem. Rev.*, 2006, **106**, 4044-4098.
2. P. Gallezot, *Chem. Soc. Rev.*, 2012, **41**, 1538-1558.
3. C. David, X. Lefèbvre, C. Lefèvre, W. Demarteau and J. M. Loutz, *Prog. Org. Coat.*, 1999, **35**, 45-54.
4. G. Lligadas, J. C. Ronda, M. Galià and V. Cádiz, *Biomacromolecules*, 2010, **11**, 2825-2835.
5. A. B. Foster, P. A. Lovell and M. A. Rabjohns, *Polymer*, 2009, **50**, 1654-1670.
6. N. Kolb and M. A. R. Meier, *Eur. Polym. J.*, 2013, **49**, 843-852.

7. N. Ji, T. Zhang, M. Zheng, A. Wang, H. Wang, X. Wang and J. Chen, *Angew. Chem., Int. Ed.*, 2008, **47**, 8510-8513.
8. Z. Tai, J. Zhang, A. Wang, M. Zheng and T. Zhang, *Chem. Commun.*, 2012, **48**, 7052-7054.
9. B. Xiao, M. Zheng, J. Pang, Y. Jiang, H. Wang, R. Sun, A. Wang, X. Wang and T. Zhang, *Ind. Eng. Chem. Res.*, 2015, **54**, 5862-5869.
10. P. Werle, M. Morawietz, S. Lundmark, K. Sörensen, E. Karvinen and J. Lehtonen, *Ullmann's Encyclopedia of Industrial Chemistry*, 2012, **2**, 263.
11. D. Ding, J. Wang, J. Xi, X. Liu, G. Lu and Y. Wang, *Green Chem.*, 2014, **16**, 3846-3853.
12. D. R. Vardon, M. A. Franden, C. W. Johnson, E. M. Karp, M. T. Guarnieri, J. G. Linger, M. J. Salm, T. J. Strathmannb and G. T. Beckham, *Energy Environ. Sci.*, 2015, **8**, 617-628.
13. A. M. Ruppert, K. Weinberg and R. Palkovits, *Angew. Chem., Int. Ed.*, 2012, **51**, 2564-2601.
14. A. Osatiashtiani, A. F. Lee, M. Granollers, D. R. Brown, L. Olivi, G. Morales, J. A. Melero and K. Wilson, *ACS Catal.*, 2015, **5**, 4345-4352.
15. V. Choudhary, S. H. Mushrif, C. Ho, A. Anderko, V. Nikolakis, N. S. Marinkovic, A. I. Frenkel, S. I. Sandler and D. G. Vlachos, *J. Am. Chem. Soc.*, 2013, **135**, 3997-4006.
16. N. Shi, Q. Liu, Q. Zhang, T. Wang and L. Ma, *Green Chem.*, 2013, **15**, 1967-1974.
17. J. M. R. Gallo, D. M. Alonso, M. A. Mellmer and J. A. Dumesic, *Green Chem.*, 2013, **15**, 85-90.
18. R. J. van Putten, J. C. van der Waal, E. de Jong, C. B. Rasrendra, H. J. Heeres and J. G. de Vries, *Chem. Rev.*, 2013, **113**, 1499-1597.
19. Y. Roman-Leshkov, C. J. Barrett, Z. Y. Liu and J. A. Dumesic, *Nature*, 2007, **447**, 982-986.
20. E. R. Sacia, M. H. Deaner, Y. L. Louie and A. T. Bell, *Green Chem.*, 2015, **17**, 2393-2397.
21. B. Saha and M. M. Abu-Omar, *Green Chem.*, 2014, **16**, 24-38.
22. V. Molinari, M. Antonietti and D. Esposito, *Catal. Sci. Technol.*, 2014, **4**, 3626-3630.
23. X. Wan, C. Zhou, J. Chen, W. Deng, Q. Zhang, Y. Yang and Y. Wang, *ACS Catal.*, 2014, **4**, 2175-2185.
24. C. M. Cai, N. Nagane, R. Kumar and C. E. Wyman, *Green Chem.*, 2014, **16**, 3819-3829.
25. Y. Cheng, J. Jae, J. Shi, W. Fan and G. W. Huber, *Angew. Chem., Int. Ed.*, 2012, **51**, 1387–1390.
26. T. Buntara, S. Noel, P. H. Phua, I. Melian-Cabrera, J. G. de Vries and H. J. Heeres, *Angew. Chem., Int. Ed.*, 2011, **50**, 7083-7087.
27. T. Buntara, S. Noel, P. H. Phua, I. Melián-Cabrera, J. G. de Vries and H. J. Heeres, *Top. Catal.*, 2012, **55**, 612-619.
28. J. Tuteja, H. Choudhary, S. Nishimura and K. Ebitani, *Chemsuschem*, 2014, **7**, 96-100.
29. T. Buntara, I. Melián-Cabrera, Q. Tan, J. L. G. Fierro, M. Neurock, J. G. de Vries and H. J. Heeres, *Catal. Today*, 2013, **210**, 106-116.
30. K. Chen, S. Koso, T. Kubota, Y. Nakagawa and K. Tomishige, *ChemCatChem*, 2010, **2**, 547-555.
31. Y. Nakagawa, X. Ning, Y. Amada and K. Tomishige, *Appl. Catal. A,* 2012, **128**, 433-434.
32, Y. Nakagawa, M. Tamura and K. Tomishige, *ACS Catal*., 2013, **3**, 2655-2668.
33. S. Liu, Y. Amada, M. Tamura, Y. Nakagawa and K. Tomishige, *Catal. Sci. Technol.*, 2014, **4**, 2535-2549.
34. S. Koso, I. Furikado, A. Shimao, T. Miyazawa, K. Kunimori and K. Tomishige, *Chem. Commun.*, 2009, 2035-2037,
35. S. Koso, N. Ueda, Y. Shinmi, K. Okumura, T. Kizuka and K. Tomishige, *J. Catal.*, 2009, **267**, 89-92.
36. S. Liu, Y. Amada, M. Tamura, Y. Nakagawa and K. Tomishige, *Green Chem.*, 2014, **16**, 617-626.
37. Y. Nakagawa, Y. Shinmi, S. Koso and K. Tomishige, *J. Catal.*, 2010, **272**, 191-194.
38. M. Chia, Y. J. Pagan-Torres, D. Hibbitts, Q. Tan, H. N. Pham, A. K. Datye, M. Neurock, R. J. Davis and J. A. Dumesic, *J. Am. Chem. Soc.*, 2011, **133**, 12675-12689.
39. Y. Nakagawa, K. Takada, M. Tamura and K. Tomishige, *ACS Catal.*, 2014, **4**, 2718-2726.
40. J. Chen, R. Liu, Y. Guo, L. Chen and H. Gao, *ACS Catal.*, 2015, **5**, 722-733.
41. M. Tamura, K. Tokonami, Y. Nakagawa and K. Tomishige, *Chem. Commun.*, 2013, **49**, 7034-7036.
42. Y. Nakagawa and K. Tomishige, *Catal. Commun.*, 2010, **12**, 154-156.
43. S. Minakata and M. Komatsu, *Chem. Rev.*, 2009, **109**, 711–724.
44. G. W. Huber, J. N. Chheda, C. J. Barrett and J. A. Dumesic, *Science*, 2005, **308**, 1446-1450.
45. L. R. Merte, G. Peng, R. Bechstein, F. Rieboldt, C. A. Farberow, L. C. Grabow, W. Kudernatsch, S. Wendt, E. Lægsgaard, M. Mavrikakis and F. Besenbacher, *Science*, 2012, **336**, 889-893.
46. M. Stoyanova, U. Rodemerck, U. Bentrup, U. Dingerdissen, D. Linke, R. W. Mayer, H. G. J. Lansink Rotgerink and T. Tacke, *Appl. Catal., A*, 2008, **340**, 242-249.
47. G. Busca, *Phys. Chem. Chem. Phys.*, 1999, **1**, 723-736.
48. W. N. P. van der Graaff, G. Li, B. Mezari, E. A. Pidko and E. J. M. Hensen, *ChemCatChem*, 2015, **7**, 1152-1160.
49. Y. Nakagawa, K. Mori, K. Chen, Y. Amada, M. Tamura and K. Tomishige, *Appl. Catal., A*, 2013, **468**, 418-425.
50. Y. Amada, Y. Shinmi, S. Koso, T. Kubota, Y. Nakagawa and K. Tomishige, *Appl. Catal., B*, 2011, **105**, 117-127.
51. Y. Amada, H. Watanabe, M. Tamura, Y. Nakagawa, K. Okumura and K. Tomishige, *J. Phys. Chem. C*, 2012, **116**, 23503-23514.
52. S. Koso, Y. Nakagawa and K. Tomishige, *J. Catal.*, 2011, **280**, 221-229.
53. J. He, C. Zhao and J. A. Lercher, *J. Am. Chem. Soc.*, 2012, **134**, 20768-20775.